Non-Linear and Chaotic Behavior of a Magnetically Levitated Doubly-Clamped Beam

Azadeh MaroufMashat
Department of Mechanical Engineering
Sharif University of Technology
Iran
Azadeh.mashat@gmail.com

Zohreh Mohammadi
Department of Mechanical Engineering
Sharif University of Technology
Iran
Zohreh_mohammadi@mech.sharif.edu

Hassan Salarieh
Department of Mechanical Engineering
Sharif University of Technology
Iran
salarieh@mech.sharif.edu

Aria Alasty
Department of Mechanical Engineering
Sharif University of Technology
Iran
aalasti@sharif.edu

Abstract
In this paper, chaotic vibrations of a doubly clamped Euler-Bernoulli beam under magnetic excitation is being investigated. First by using the Galerkin Method the governing ordinary differential equations of vibrations of the beam at time space is extracted. Then nonlinear dynamics and chaos is studied by using the Poincare map. Existence of third order periodic orbit is indicated in the system by the means of simulation and finally it is concluded that there is chaos in the system according to the Li-Yorke theorem.

Key Words
Doubly clamped Beam, Chaos, Magnetic excitation

1. Introduction

Vibrations under electro-magnetic excitation may introduce nonlinear phenomena such as sub-harmonic, super-harmonic oscillations and chaos. In using extended Kalman filtering method, the nonlinear force of an electromagnet on a single clamped beam is identified. In that work, it is shown that harmonic excitation on a clamped elastic beam may result in super-harmonic behavior and irregular response. Electro-magnetic excitation has many applications in active magnetic bearing systems. In using a nonlinear model of electromagnetic force which can justify the chaotic response of one-dimensional magnetic levitation systems, has been proposed. Using an experimental setup, Chang and Tung showed the chaotic response for magnetic bearing system in high frequency range (30 to 40 Hz). Instead of a multiplicative form they have identified a superlative form for electromagnetic force model. In experimental and analytical studies are performed on chaotic behavior of active magnetic bearings. Investigation of chaos in magnetically levitated doubly clamped beams is examined via analytical and experimental methods in.

In this paper, the behavior of a doubly clamped beam under magnetic excitation is studied. The results of this research are widely used in MEMS, actuation mechanisms in small manipulators, guiding precision tool (instrument) machines, and also in high frequency oscillating switches.

2. Governing equations of the beam under magnetic excitation

The experimented beam is supposed to be an Euler-Bernoulli one, as it is cleared in Fig. 1, it is excited with the electro-magnetic force.

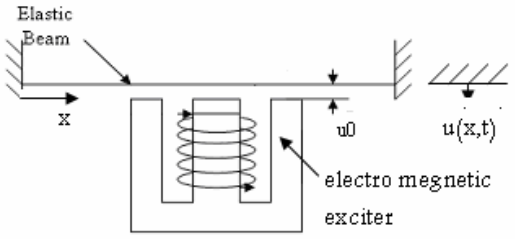

Figure1- schematic of the experimented beam

In many of nonlinear investigations, the nonlinear electromagnetic force has been assumed proportional to the coil current squared and inversely proportional to the gap squared. This magnetic force model is suitable in ideal case, where the electromagnetic losses, flux leakage and saturation of iron which may exist in real applications, are ignored. The electro-magnetic force which is used here is modeled as:

$$Fe\delta(x-\frac{l}{2})=\frac{k(I\sin(\omega t)+I_0)^2}{(u-u_0)^2}\delta(x-\frac{l}{2}) \qquad (1)$$

Where ω is the exciting frequency of magnetic force, I is the current of oscillating force, I_0 is initial current of excitation (bias), u is the lateral vibrations of the beam, u_0 denotes the air gap between the magnetic head and the mid point of the beam, $\delta(.)$ is the Dirac delta function: $\delta(x-\frac{l}{2})$ shows that the electromagnetic force is exerted in the mid point of the

beam, and k is a coefficient with dimension of $\frac{Nm^2}{Ampere^2}$.

Since the studied beam is a doubly clamped beam, so the boundary conditions are obtained as:

$$\begin{cases} u(0.t)=0 \\ u_x(0,t)=0 \\ u(l,t)=0 \\ u_x(l,t)=0 \end{cases} \quad (2)$$

The governing equation of a doubly clamped Euler-Bernoulli beam with linear damping is given by:

$$mu_{tt}+EJu_{xxxx}+\Gamma u_t = Fe\,\delta(x-\frac{l}{2}) \quad (3)$$

Where Γ the damping coefficient, m is the mass per length of the studied beam, E is the elasticity module and J is the second order moment of surface around the null axis.

To obtain the governing ODE of the system by the Galerkin projection method, first we should find the linear shape functions of equation (3). To this end we set the right-hand side of equation (3) to zero

$$mu_{tt}+EJu_{xxxx}+\Gamma u_t = 0 \quad (4)$$

Using the following definition

$$C=\sqrt{\frac{EJ}{m}} \quad (5)$$

Eq. (4) is rewritten as:

$$C^2u_{xxxx}+u_{tt}+\frac{\Gamma}{m}u_t=0 \quad (6)$$

By using the method of separation of variables the eigen functions or the shape functions of the above equation are obtained as:

$$\begin{aligned} X_n(x) = & \frac{-\cos(\lambda_n l)+\cosh(\lambda_n l)}{\sin(\lambda_n l)-\sinh(\lambda_n l)}\sin(\lambda_n x) \\ & +\cos(\lambda_n x) \\ & -\frac{-\cos(\lambda_n l)+\cosh(\lambda_n l)}{\sin(\lambda_n l)-\sinh(\lambda_n l)}\sinh(\lambda_n x) \\ & -\cosh(\lambda_n x) \end{aligned} \quad (7)$$

Where λ_n is the nth eigen value of the system which is calculated from the below equation:

$$\cos(\lambda l)\cosh(\lambda l)=1 \quad (8)$$

Natural frequency of the system is defined as

$$\omega_n = C\lambda^2=\sqrt{\frac{EI}{m}}\lambda^2 \quad (9)$$

So u as a function of x and t is written as

$$u(x,t)=\sum_{i=1}^{n}A_iX_i(x)T_i(t) \quad (10)$$

To simplify equation (1), the first 5 terms of the Taylor expansion formula is used for Galerkin projection of Eq. (3).

$$\frac{1}{(u-u_0)^2}=\frac{1}{u_0}\left(\frac{1}{u_0}+2\frac{u}{u_0^2}+3\frac{u^2}{u_0^3}+4\frac{u^3}{u_0^4}+\frac{5u^4}{u_0^6}+...\right) \quad (11)$$

$$F_e(x,t)=k(I\sin(\omega t)+I_0)^2\delta(x-\frac{l}{2})\left(\frac{1}{u_0^2}+\frac{2u}{u_0^3}+\frac{3u^2}{u_0^4}+\frac{4u^3}{u_0^5}+\frac{5u^4}{u_0^6}\right)$$

It must be noted that one can use Eq. (1) for Galerkin projection directly; however this results in a complicated ODE equation which is not useful for analytical studies.

Now substituting Equations (10) and (11) into Equation (3) we obtain:

$$\begin{aligned} & \sum_{n=1}m\ddot{T}_n(t)X_n(x)+\sum_{n=1}EJX_n''''T_n(t)+\sum_{n=1}\Gamma\dot{T}_n(t)X_n(x) \\ & =k(I\sin(\omega t)+I_0)^2\delta(x-\frac{l}{2})\left(\frac{1}{u_0^2}+\frac{2u}{u_0^3}+\frac{3u^2}{u_0^4}+\frac{4u^3}{u_0^5}+\frac{5u^4}{u_0^6}\right) \end{aligned} \quad (12)$$

The first term of Equation (10) are used to approximate the governing equation of the first mode vibration of beam.

$$u(x,t)=X_1(x)T_1(t) \quad (13)$$

Multiplying both sides of Equation (12) by $X_1(x)$ and integrating from 0 to l we obtain

$$\begin{aligned} & m\ddot{T}_1(t)\int_0^l X_1^2(x)dx+EJT_1(t)\lambda_1^4\int_0^l X_1^2(x)dx+\Gamma\dot{T}_1(t)\int_0^l X_1^2(x)dx= \\ & \int_0^l k(I\sin(\omega t)+I_0)^2\delta(x-\frac{l}{2}) \\ & \left(\frac{X_1(x)}{u_0^2}+\frac{2T_1X_1^2(x)}{u_0^3}+\frac{3T_1^2X_1^3(x)}{u_0^4}+\frac{4T_1^3X_1^4(x)}{u_0^5}+\frac{5T_1^4X_1^5(x)}{u_0^6}\right) \end{aligned} \quad (14)$$

Where for the above first mode of vibration, $\Gamma=2\xi\omega_1 m$, and ξ is the damping factor.

Considering the first two terms of Equation (14) we have

$$u(x,t)=X_1(x)T_1(t)+X_2(x)T_2(t) \quad (15)$$

Multiplying both sides of Equation (12) by $X_1(x)$ and $X_2(x)$ and then integrating from 0 to l we obtain:

$$\begin{aligned} & m\ddot{T}_1(t)\int_0^l X_1^2(x)dx+EJT_1(t)\lambda_1^4\int_0^l X_1^2(x)dx+\Gamma\dot{T}_1(t)\int_0^l X_1^2(x)dx= \\ & =k(I\sin(\omega t)+I_0)^2\delta(x-\frac{l}{2})\left(\frac{1}{u_0^2}X_1(x)+\frac{2u}{u_0^3}X_1(x)+\frac{3u^2}{u_0^4}X_1(x)+\frac{4u^3}{u_0^5}X_1(x)+\frac{5u^4}{u_0^6}X_1(x)\right) \\ & m\ddot{T}_2(t)\int_0^l X_2^2(x)dx+EJT_2(t)\lambda_2^4\int_0^l X_2^2(x)dx+\Gamma\dot{T}_1(t)\int_0^l X_2^2(x)dx= \\ & =k(I\sin(\omega t)+I_0)^2\delta(x-\frac{l}{2})\left(\frac{1}{u_0^2}X_2(x)+\frac{2u}{u_0^3}X_2(x)+\frac{3u^2}{u_0^4}X_2(x)+\frac{4u^3}{u_0^5}X_2(x)+\frac{5u^4}{u_0^6}X_2(x)\right) \end{aligned} \quad (16)$$

3. Dimensionless Equations

To apply numerical simulations, it is better that the dimensionless governing equations of the system are obtained. To this end, the following non-dimension parameters are defined:

$$\mu = \frac{u}{u_0}, X = \frac{x}{l}, \tau = \omega_1 t \tag{17}$$

Where μ, X , and τ are dimensionless transversal displacement, coordinate and time respectively; and ω_1 is the first mode natural frequency of the system.

μ can also be written as

$$\mu(x,\tau) = \sum_{i=1}^{n} X_i(X) T_i(\tau) \tag{18}$$

So we have

$$u_{tt} = \omega_1^2 u_0 \mu_{\tau\tau}, u_{xxxx} = \frac{u_0}{l^4} \mu_{XXXX} \tag{19}$$

$$Fe\delta(X - \frac{1}{2}) = \tag{20}$$

$$\frac{kI_0^2(\frac{I}{I_0}\sin(\frac{\omega\tau}{\omega_1})+1)^2}{u_0^2 m}(1+2\mu+3\mu^2+4\mu^3)\delta(X-\frac{1}{2})$$

$$\lambda = \frac{g}{l}, \qquad \omega_1 = (\frac{g}{l})^2\sqrt{\frac{EJ}{m}} \tag{21}$$

$$r = \frac{\omega}{\omega_1}, \quad s = \frac{I}{I_0} \tag{22}$$

Where r is the ratio of the first linear natural frequency of the system to the exciting frequency of the system; and s is the ratio of excitation current to the bias current.

Equation (3) will be written as:

$$\frac{\mu_{XXXX}}{g^4} + \mu_{\tau\tau} + 2\xi\mu_{\tau} = \tag{23}$$

$$\frac{kI_0^2(s\sin(r\tau)+1)^2}{\omega_1^2 u_0^3 m}(1+2\mu+3\mu^2+4\mu^3+5\mu^4)\delta(X-\frac{1}{2})$$

Getting the first one term of the Eq. (18), and applying the Galerkin method, it is obtained that

$$\ddot{T}_1(\tau)\int_0^1 X_1^2(X)dX + T_1(\tau)\int_0^1 X_1^2(X)dX + 2\xi\dot{T}_1(t)\int_0^1 X_1^2(X)dX$$
$$= \int_0^1 \frac{kI_0^2(s\sin(r\tau)+1)^2}{\omega_1^2 u_0^3 m}\delta(X-\frac{1}{2})(1+2X_1^2T_1+3X_1^3T_1^2+4X_1^4T_1^3+5X_1^5T_1^4)dx \tag{24}$$

Using the same method equation (16) is written in the following non-dimension forms as:

$$\ddot{T}_1\int_0^1 X_1^2 dX + T_1\int_0^1 X_1^2 dX + \dot{T}_1\int_0^1 X_1^2 dX \tag{25}$$
$$= \int_0^1 \frac{kI_0^2(s\sin(r\tau)+1)^2}{\omega_1^2 u_0^3 m}\delta(x-\frac{l}{2})(1+2\mu X_1+3\mu^2 X_1+4\mu^3 X_1+5\mu^4 X_1)dX$$
$$\ddot{T}_2\int_0^1 X_2^2 dX + T_2\int_0^1 X_2^2 dX + \dot{T}_2\int_0^1 X_2^2 dX$$
$$= \int_0^1 \frac{kI_0^2(s\sin(r\tau)+1)^2}{\omega_1^2 u_0^3 m}\delta(x-\frac{l}{2})(1+2\mu X_2+3\mu^2 X_2+4\mu^3 X_2+5\mu^4 X_2)dX$$

Suppose $K_1 = \int_0^1 X_1^2 dX$, $K_2 = \int_0^1 X_2^2 dX$

We can simplify Eq. (24) and (25) as

$$K_1(\ddot{T}_1(\tau)+T_1(\tau)+2\xi\dot{T}_1(t)) \tag{26}$$

$$\int_0^1 \frac{kI_0^2(s\sin(r\tau)+1)^2}{\omega_1^2 u_0^3 m}\delta(X-\frac{1}{2})(1+2X_1^2T_1+3X_1^3T_1^2+4X_1^4T_1^3+5X_1^5$$

$$K_1(\ddot{T}_1+T_1+\dot{T}_1) = \frac{kI_0^2(s\sin(r\tau)+1)^2}{\omega_1^2 u_0^3 m}\times \tag{27}$$
$$(1+2\mu X_1(\frac{1}{2})+3\mu^2 X_1(\frac{1}{2})+4\mu^3 X_1(\frac{1}{2})+5\mu^4 X_1(\frac{1}{2}))$$
$$K_2(\ddot{T}_2+T_2+\dot{T}_2) = \frac{kI_0^2(s\sin(r\tau)+1)^2}{\omega_1^2 u_0^3 m}\times$$
$$(1+2\mu X_2(\frac{1}{2})+3\mu^2 X_2(\frac{1}{2})+4\mu^3 X_2(\frac{1}{2})+5\mu^4 X_2(\frac{1}{2}))$$

4. Simulation and Results

Equations (26) and (27) can be analytically investigated by using perturbation methods. This would reveal the character of the regular (non-chaotic) responses to expect, as a "background" for the cases of chaos observed. However here we consider the numerical solutions of (26) and (27).

Using the numerical methods the Equations derived in section (3) are solved to plot the time series presenting the response of the midpoint of the doubly clamped beam under harmonic excitations. Different excitation frequencies and different bias currents are examined during various simulations. Besides, the Poincare maps of the collected data are plotted to investigate the existence of regular and irregular responses.

To plot the Poincare map of the response, the first 1000 points are considered as the initial transient data and hence are omitted. The Poincare map is constructed by sampling the time series with $2\pi/r$ - period, where r is the non-dimensional excitation frequency.

In these simulations, we set $s = 1$, and for different values of excitation frequencies and bias currents, the time series of responses are obtained and for each of them, the Poincare map are plotted. The first, the second and the third order harmonic responses are obtained using Poincare map analysis. Different values of bias currents which are considered for numerical simulations are: 500, 1700, 1800 and 2000 (mA) .

For each of the currents mentioned above, wide ranges of excitation frequencies from very small values to large values are examined for nonlinear, regular and irregular behavior. In what follows some of these time series and Poincare maps are presented.

It was observed that for the bias current of $500\ mA$ the Poincare section has always a single point. An example of these diagrams is shown in Fig. (2). The single point on the Poincare map shows that the response is periodic and its period is equal to the excitation period, i.e. $2\pi/r$.

In Fig. (3), it is observed that for the bias current of 1700 mA the Poincare section has two fixed points.

For the excitation current of 1700 mA the Poincare map has only a single fixed point for the frequencies up to 19 Hz, two points, i.e. a second order fixed point, for the frequencies from 19 Hz to 20.04 Hz, a single point for the frequencies from 20.04 Hz to 53 Hz, two points for the frequencies from 53 Hz to 137 Hz and again a single point for the frequencies higher than 137 Hz.

When the bias current is 1800 mA, the Poincare section is observed to be a single point for low frequencies up to 18 Hz; two points for the frequencies form 19 Hz to 33 Hz; a single fixed point for the frequencies from 34 Hz to 52 Hz; two fixed points for the frequencies from 52 Hz to 65 Hz; a single fixed point for the frequencies up to 136 Hz; two fixed points for frequencies of 137 to 138 Hz, and finally a single point for higher frequencies. Figure (4) shows the times series and Poincare map of one simulation for $I_0 = 1800\ mA$.

For 2000 mA bias current, when the excitation frequency is lower than 12.9 Hz, the Poincare map has a single fixed point. For higher frequencies up to 13.12 Hz, the single fixed point is substituted by a third order one, which results in chaotic response regarding the Li-Yorke theorem. After that, up to 13.5 Hz, a single fixed point is constructed, then a second order fixed point is observed for the frequencies from 13.5 Hz of 18.5 Hz. For the frequencies from 18.5 Hz to 40 Hz a single fixed point, and for the frequencies of 41 to 42 Hz, a second order point are observed. Finally, a single point for the frequencies from 42 to 141 Hz and two points for the frequencies from 142 to 150 Hz are constructed on the Poincare sections.

One of these simulations is presented in Fig. (5).

5. Conclusion

In this paper nonlinear vibrations of a doubly clamped beam under electromagnetic excitation is investigated theoretically and the existence of chaos is also studied. At first, the governing equations of a doubly clamped beam is derived and then the nonlinear term of electromagnetic force is inserted in the equations and by using the Galerkin method the equations are reformed into ordinary differential equations. Using numerical methods, the Poincare maps based on the vibrations of the midpoint of the beam are obtained. The first, the second and the third order sub-harmonic responses of the system are observed. According to the Li-Yorke Theorem the existence of the third order sub-harmonic response in the system guarantees the existence of aperiodic and hence topological chaos in the system.

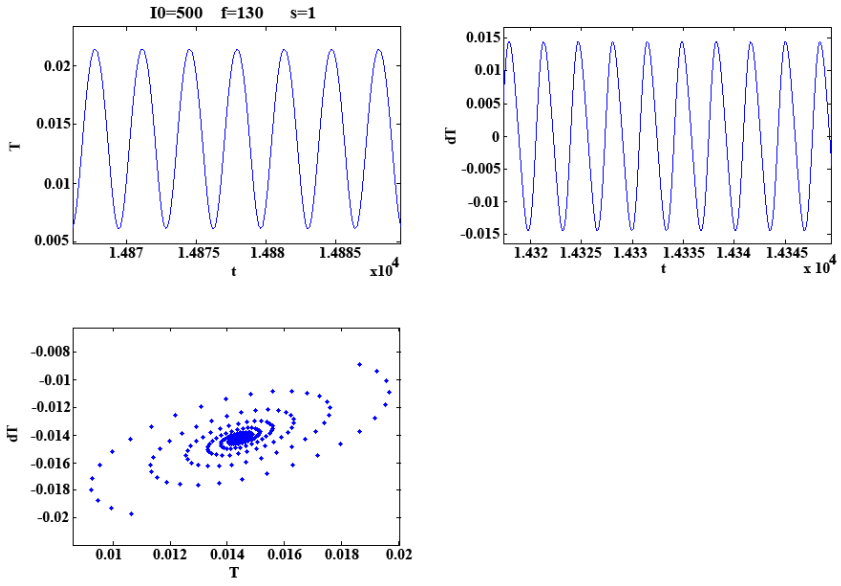

Figure 2[1]. Time history of vibrations of the beam and Poincare diagram for $I = 500\ mA$, $f = 60\ Hz$, $s = 1$

[1] dT is derivation of T

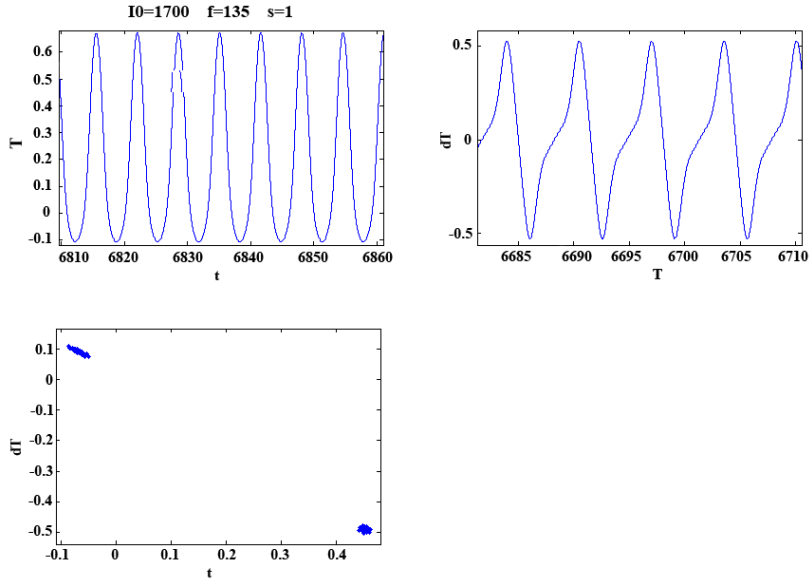

Figure 3. Time history of vibrations of the beam and Poincare diagram for $I = 1700\ mA$, $f = 135\ Hz$, $s = 1$

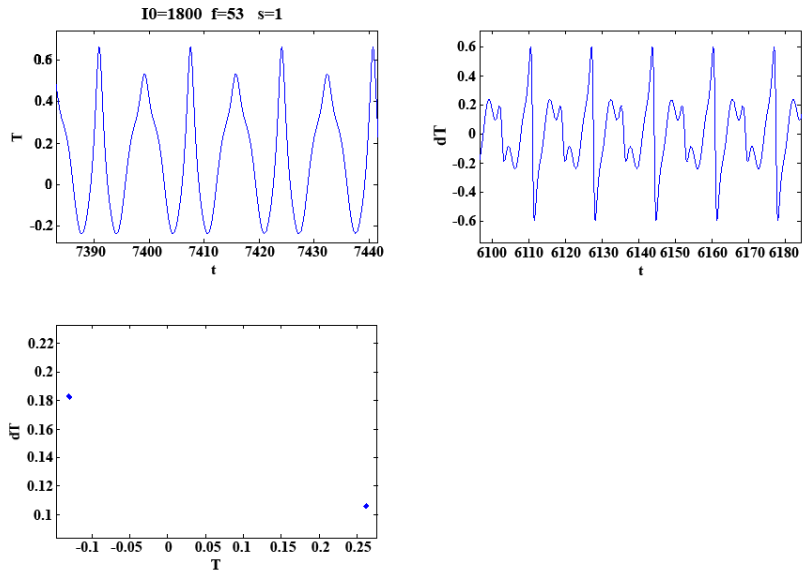

Figure 4. Time history of vibrations of the beam and Poincare diagram for $I = 1800\ mA$, $f = 53\ Hz$, $s = 1$

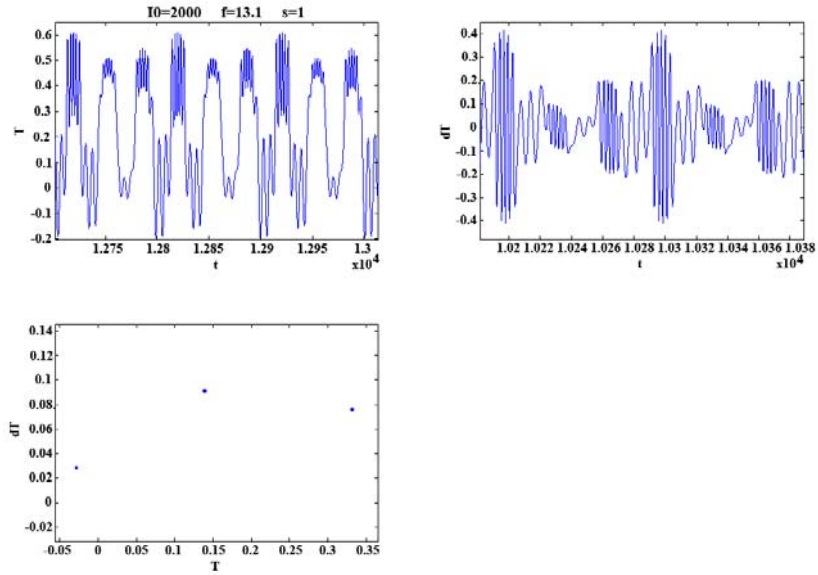

Figure 5. Time history of vibrations of the beam and Poincare diagram for $I = 2000\ mA$, $f = 13.1\ Hz$, $s = 1$

Refrence

A. Alasty (2006), R. Shabani, Nonlinear parametric identification of magnetic bearings, *Mechatronics* 16: 451-459.

J. Argyris, G. Faust, M. Haase (1994), *An Exploration of Chaos*, North Holland.

Chang S. C. and Tung P.C (1998), Identification of a non-linear electromagnetic system: *An experimental study*, *Journal of Sound and Vibration* 214:853-871.

S-C. Chang, H-P. Lin (2005), *Non-linear dynamics and chaos control for an electromagnetic system*, *Sound and Vibration* 279: 327-344.

H. Haberman and G. L. Liard (1979), Practical Magnetic Bearings, *IEEE Spectrum*, Sep. 26-32.

J.I. Hussain (2007), Chaos via torus breakdown in the vibration response of a rigid rotor supported by active magnetic bearings, *Chaos Solitons Fractals* 31: 912-927.

A.M. Mohamed and F.P. Emad (1993), Nonlinear Oscillations in Magnetic Bearing Systems, *IEEE Transactions on Automatic Control* 38.

Lawrence Perko (1991), *Differential Equations and Dynamical Systems*, Springer-Veriage New York, Inc.

R. Shabani R., H. Salarieh, A. Alasty (2006), Comments on "Identification of a nonlinear electromagnetic system: An experimental study, *Journal of sound and Vibrations* 290:1333-1334.

R. Shabani (2006), Investigating dynamical behavior identification and control of magnetic bearings, *PHD thesis, Mechanical Engineering Department, Sharif University of Technology, Tehran, Iran*, July.

Tyn Myint U (1987), *Partial Differential Equation of Mathematical Physics*, 2nd Edition, North Holland, New York, Amsterdam, Oxford.

L. Wei, S.A. Kah, H. Ruilong (2007), Vibration analysis of a ferromagnetic plate subjected to an inclined magnetic field, *International Journal of Mechanical Sciences* 49: 440-446.

Z. Mohammadi, A. M. Mashat (2007), Investigating non-linear and chaotic behavior of a doubly-clamped beam with electromagnetic exciter theoretically and experimentally, *BSc. dissertation, Department of Mechanical Engineering, Sharif university of technology, Tehran, Iran*. August